Behavioral/Systems/Cognitive

Cingulum Microstructure Predicts Cognitive Control in Older Age and Mild Cognitive Impairment

Claudia Metzler-Baddeley,[1] Derek K. Jones,[1] Jessica Steventon,[1] Laura Westacott,[1] John P. Aggleton,[1] and Michael J. O'Sullivan[1,2]

[1]Cardiff University Brain Research Imaging Centre (CUBRIC), School of Psychology, and the Neuroscience and Mental Health Research Institute, Cardiff University, Cardiff CF10 3AT, United Kingdom, and [2]Department of Clinical Neuroscience, Institute of Psychiatry, King's College London, London SE5 8AF, United Kingdom

Cognitive control, an important facet of human cognition, provides flexibility in response to varying behavioral demands. Previous work has focused on the role of prefrontal cortex, notably the anterior cingulate cortex. However, it is now clear that this is one node of a distributed cognitive network. In this emerging network view, structural connections are inherent elements, but their role has not been emphasized. Furthermore, lesion and functional imaging studies have contributed little knowledge about anatomical segregation, functional specialization, and behavioral importance of white matter connections. The relationship between cognitive control and microstructure of connections within the cingulum, a major white matter tract and conduit of projections to prefrontal sites, was probed *in vivo* in humans with diffusion MRI. Twenty healthy controls and 25 individuals with amnestic mild cognitive impairment (MCI), an early stage of age-associated cognitive deterioration, underwent cognitive testing, including several measures of cognitive control. For each individual, the anterior, middle, posterior, and parahippocampal portions of the cingulum bundle were reconstructed separately using deterministic tractography and anatomical landmarks. Microstructural variation in the left anterior cingulum was closely related to interindividual control based on verbal or symbolic rules. Errors in a task that involved maintenance of spatial rules were largely restricted to patients with MCI and were related, additionally, to right anterior cingulum microstructure. Cognitive control in MCI was also independently related to posterior parahippocampal connections. These results show how specific subpopulations of connections are critical in cognitive control and illustrate fine-grained anatomical specializations in the white matter infrastructure of this network.

Introduction

Cognitive control enables such quintessential aspects of human cognition as reasoning, problem solving, and behavioral flexibility (Miller, 2000). Functional MRI and brain injury studies underline the importance of dorsal and medial prefrontal cortex regions (Miller, 2000; Alexander et al., 2007) but also illustrate that these regions act within distributed networks (Dosenbach et al., 2006). An untested prediction is that the status of prefrontal white matter connectivity contributes to efficacy of executive control functions, a relationship that should hold only for specific connections, as control relies on a subset of prefrontal sites.

The cingulum is a frontal association tract that could play a critical role because it connects sites repeatedly implicated in cognitive control. A chief example is the adjacent anterior cingu-late cortex, specifically the dorsal portion (dACC), which is involved in the control of goal-directed behavior (Rushworth et al., 2003; Holroyd and Yeung, 2012). In fMRI studies, the dACC is implicated in networks for top-down control of attention, particularly instantiating and maintaining "task set" (Dosenbach et al., 2006), a set of rules that governs the possible relationships between stimuli and responses, and, therefore, flexible responding to individual stimuli. Neuropsychological tests, such as Digit Symbol Substitution, Stroop Suppression, Tower of London, and fluency tasks, all tax "task set" by instructing participants to respond according to a given set of rules, which remains until task completion. If cognitive control depends on rapid communication between dACC and a wider network, then cingulum microstructure should prove crucial.

The cingulum contains prominent medial and dorsal prefrontal connections, including those of the anterior cingulate cortex with the medial parietal and temporal lobes. However, the cingulum harbors several other populations of association fibers of varying lengths, leading to changing patterns of connectivity along its rostrocaudal extent that mirror functional segregation along the cingulate gyrus (Vogt et al., 1992). For example, while dACC is implicated in networks for top-down attentional control and goal-directed behavior, the retrosplenial cortex, which is also connected via the cingulum, is implicated in scene learning and episodic memory (Vann et al., 2009). A major prediction, therefore, is that rostral parts of the cingulum will be most consistently

Table 1. Demographics and group comparisons of cognitive scores

	Controls	MCI	Group comparison
Years of age	74 (6.5)	76.8 (7.3)	$t_{(43)} = -1.3; p = 0.19$
Years of education	15 (2.8)	14 (3.7)	$t_{(43)} = 1.8; p = 0.08$
NART-R IQ	120 (9.0)	115 (10.8)	$t_{(43)} = 1.8; p = 0.08$
Percentage females	50%	44%	
Percentage right-handed	95%	100%	
Digit Symbol Substitution Test total	56.7 (18.6)	34.8 (11.9)	$t_{(40)} = 4.6; p \leq 0.001^{a}$
Stroop suppression	96.1 (15.7)	57.4 (28.2)	$t_{(39)} = 5.2; p \leq 0.001^{a}$
Tower of London rule violations	1.2 (1.7)	5.8 (4.5)	$t_{(41)} = -4.2; p \leq 0.001^{a}$
Category fluency	39.5 (10.1)	25.6 (7.9)	$t_{(41)} = 4.8; p \leq 0.001^{a}$
Verbal fluency	43.2 (14.1)	35.9 (11.3)	$t_{(41)} = 1.8; p = 0.07$
Trails switching cost	74 (31.5)	105.4 (50.7)	$t_{(42)} = -2.1; p = 0.05$
Verbal span	10.35 (1.84)	9.6 (2.1)	$t_{(43)} = 1.4; p = 0.19$
Visual span	6.8 (1.7)	4.2 (1.3)	$t_{(41)} = 5.7; p \leq 0.001^{a}$
Processing speed	45.1 (8.7)	52.2 (11.3)	$t_{(41)} = -2.2; p = 0.03$

Scores are shown as mean (SD). Verbal short-term memory span was assessed with the Digit Span Task; visual span was assessed with the Visual Pattern Test; and processing speed was measured as the average response time in the Stroop and the Verbal Trails baseline conditions.

[a]Bonferonni-corrected ($p \leq 0.004$) significant group differences.

associated with control processes, while the parahippocampal cingulum (PHC) will show little relationship given its preponderance of temporal and parietal interconnections.

Using two complementary approaches, we tested the prediction that the efficacy of control functions would depend on specific connections. First, we related cognitive control to within tract variation in microstructure by comparing relationships with different segments of the cingulum, which vary in the number and destination of prefrontal fibers. To study potential functional subdivisions, the bundle was partitioned into three dorsal segments (anterior, middle, and posterior) and a ventral parahippocampal portion. Second, we performed comparisons between tracts, contrasting the cingulum with the fornix. The fornix also connects to prefrontal cortex but innervates different subregions (Poletti and Creswell, 1977). Finally, by extending the analysis to a clinical group, we exploited variations introduced by early cognitive decline to gain additional insights into the connectional anatomy of cognitive control.

Materials and Methods

Participants

Healthy older participants were recruited from the local community by advertisements posted in family physician waiting rooms, by newsletters and mailshots, and via the School of Psychology Community Panel of healthy research volunteers at Cardiff University. The 20 healthy control participants (10 males and 10 females) of the present study were a subgroup of a sample of 46 individuals who were between the ages of 53 and 93 years and who were recruited for an aging study (Metzler-Baddeley et al., 2011). A subgroup was selected to provide optimal matching with the mild cognitive impairment (MCI) group. To help match the patient and control groups for age and intelligence, only those healthy participants over the age of 65 years (the MCI group were all over 65) and with a verbal IQ not exceeding two SDs above the average patient IQ in the National Adult Reading Test Revised (NART-R) were included. The selection of this subgroup was based entirely on demographic variables and verbal intelligence, and was blind to their cognitive scores and imaging data.

Twenty-five patients with MCI were recruited from the Cardiff Memory Clinic (14 males and 11 females). All patients underwent a standard memory clinic assessment, including clinical history, ascertainment of vascular risk factors, full neurological examination, basic hematology and biochemistry investigations, neuroimaging with CT or MRI, and cognitive screening with the Addenbrooke's Cognitive Examination (ACE) (Mioshi et al., 2006). Diagnosis of MCI was based on established current criteria (Albert et al., 2011). Objective memory impairment was confirmed by a score >1.5 SDs below age-matched controls on either the ACE verbal memory subscore or the visual memory test from the Repeat-

able Battery for the Assessment of Neurological Status. All patients had a Mini Mental State Examination score of ≥24 (mean, 26; SD, 1.7) and a Clinical Dementia Rating of 0.5 (Morris, 1993). Consecutive patients who were assessed by a single neurologist (M.J.O.) and who were eligible and willing to take part were recruited.

Exclusion criteria for both groups were as follows: previous moderate-to-severe head injury; prior or current alcohol and/or drug abuse (as defined by Diagnostic and Statistical Manual of Mental Disorders); previous large-artery or disabling stroke or cerebral hemorrhage; known peripheral, cervical, or coronary artery disease; structural heart disease or heart failure; and contraindications to MRI. In addition, no patient with MCI met diagnostic criteria or had characteristic cognitive or behavioral features to suggest other degenerative disorders, such as the frontotemporal lobar degenerations, corticobasal degeneration, or dementia with Lewy bodies. An additional exclusion criterion for healthy participants was evidence of previous memory symptoms. Detailed background cognitive information of the whole aging sample has been reported previously (Metzler-Baddeley et al., 2011). Basic demographic information and cognitive test scores for the participants can be found in Table 1.

MRI acquisition

Diffusion-weighted MR data were acquired using a 3 T GE HDx MRI system (General Electric) with a twice-refocused spin-echo echo-planar imaging sequence providing whole oblique axial (parallel to the commissural plane) brain coverage. Data acquisition was peripherally gated to the cardiac cycle. Data were acquired from 60 slices of 2.4 mm thickness, with a field of view of 23 cm, and an acquisition matrix of 96 × 96. TE (echo delay time) was 87 ms and parallel imaging [array spatial sensitivity encoding (ASSET) factor, 2] was used. The b-value was 1200 s/mm^2. In each imaging session, data were acquired with diffusion encoded along 30 isotropically distributed orientations and three nondiffusion-weighted scans according to an optimized gradient vector scheme. The acquisition time was ~13 min. The acquired images were corrected for distortions, introduced by the diffusion-weighting gradients, and for subject motion with appropriate reorienting of the encoding vectors (Leemans and Jones, 2009). Image voxels around the fornix are particularly susceptible to CSF contamination and hence partial volume artifacts (Metzler-Baddeley et al., 2012). In the presence of tissue atrophy due to neurodegeneration and aging, partial volume error is a critical methodological issue. The free water elimination approach (Pasternak et al., 2009) was used to correct for atrophy-related partial volume effects before fitting a tensor model to the data in each voxel to estimate the diffusion orientation and to yield quantitative metrics of fractional anisotropy (FA) and mean diffusivity (MD).

Cognitive assessment

All participants underwent detailed cognitive assessment over two 1.5 h testing sessions (Table 1) (Metzler-Baddeley et al., 2011). Verbal intelli-
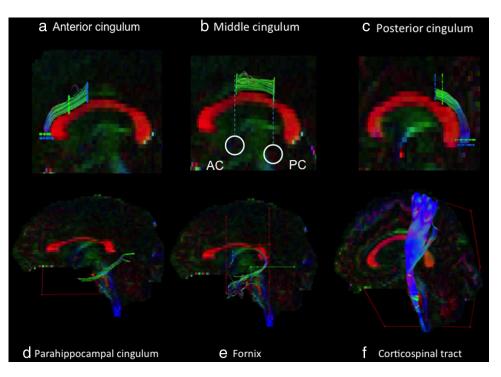
Figure 1. Reconstructions of white matter tracts. *a–f*, Tractography using ROI waypoints (seed point ROIs, blue; AND ROIs, green; NOT ROIs, red) for the anterior cingulum (*a*), middle cingulum (*b*), posterior cingulum (*c*), PHC (*d*), fornix (*e*), and corticospinal tract (*f*) in the native space of one participant. AC, anterior commissure; PC, posterior commissure.

gence was estimated with the NART-R. Verbal working memory span was assessed with the Digit Span forwards task from the Wechsler Adult Intelligence Scale, Third UK Edition (WAIS-III). Visual memory span was assessed with the Visual Pattern Test. Different aspects of cognitive control were assessed in tasks that all required the maintenance of a task set under speeded response conditions: attention switching was examined with a version of the verbal trails test that required alternation between letters and digits. This task allows the measurement of response times costs in the switching condition relative to a baseline condition in which participants generate blocks of letter and digit sequences separately. The suppression of response-incongruent information was assessed with the Color-Word Stroop test. Problem-solving skills and violation of task set rules were assessed with the Tower of London test from the Delis and Kaplan Executive Function System battery (D-KEFS). Verbal generation and fluency were measured with the verbal fluency tests from the D-KEFS for letters F, A, and S and for the categories of animals and boys' names. In addition, the Digit Symbol Substitution test from the WAIS-III provided a measure of focused attention and psychomotor performance. Processing speed was measured as the average response time in the baseline conditions of the Stroop test (reading of color words) and the Verbal Trails Test (generation of a letter and a digit sequence without alternations). MCI patients performed significantly worse in the Digit Symbol Substitution Task, Category Fluency, Stroop, Tower of London, and Visual Span tests but did not differ from controls in age, education, NART-IQ, verbal span, verbal fluency, verbal trails and processing speed (Table 1).

Image processing and tractography
Tractography was performed using ExploreDTI (http://www.exploreDTI.com). A deterministic tracking algorithm based on the diffusion tensor model (DTI) was used to reconstruct the four cingulum segments and the corticospinal control tract. The DTI tracking algorithm estimated the principal diffusion orientation at each seed point and propagated in 0.5 mm steps along this direction. The fiber orientations were then estimated at the new location and the tracking moved a further 0.5 mm along the direction that subtended the smallest angle to the current trajectory. In this way, a pathway was traced through the data until FA fell below a threshold of 0.15 or the direction of the pathway changed through an angle >60°. DTI-based tractography has been shown to generate ana-

tomically plausible and reproducible reconstructions of tracts within regions of coherently oriented fibers. However, DTI-based fiber tractography is less successful in reconstructing the fibers of the fornix because of its small size and close proximity to other larger white matter tracts (e.g., anterior commissure). In such settings, a technique is required that can resolve separate peaks in fiber orientation due to crossing fiber populations, and still maintain the fidelity of the tracking algorithm to the tract in question and avoid incorrect, aberrant results. Therefore, deterministic tracking based on constrained spherical deconvolution (Tournier et al., 2004), which extracts peaks in the fiber orientational density function in each voxel, was chosen as a more appropriate technique for fornix tractography. In this way, a pathway was traced through the data until the scaled height of the fiber orientation density function peak fell below 0.1 or the direction of the pathway changed through an angle >60°.

Whole-brain tractography was performed using every voxel as a seed point. Three-dimensional reconstructions of the four cingulum segments and the two control tracts (Fig. 1) were then extracted from whole-brain tractograms by applying multiple waypoint regions of interest (ROIs) masks. ROIs defined tracts based on Boolean logical operations (e.g., selecting fibers that traversed ROI-1 and ROI-2 but not ROI-3). Representative ROIs for the five tracts are shown in Figure 1 with seed point OR ROIs depicted in blue, AND ROIs in green, and NOT ROIs in red. All ROIs were manually drawn in native space on color-coded fiber-orientation maps for each individual dataset by three operators (C.M.-B., L.W., J.S.) blinded to the participants' ages and cognitive scores. The parahippocampal portion of the cingulum, the fornix, and the corticospinal tracts were reconstructed using landmark techniques that have previously been shown to be highly reproducible. To reconstruct the anterior, middle, and posterior portions of the cingulum, a landmark-based tractography protocol was developed and assessed for reproducibility. The mean FA and MD (derived from the free water-corrected tensors) were then calculated for all reconstructed pathways in ExploreDTI by averaging the values sampled at each 0.5 mm step along the pathways. In this way, tract-specific means of FA and MD were obtained for the four cingulum segments and the corticospinal tract on both left and right hemispheres, as well as for the fornix tract.

Reconstruction of cingulum and cingulum segments
The anterior, middle, and posterior segments of the cingulum were defined by using the anterior and posterior commissure as anatomical landmarks (Jones et al., 2006) (Fig. 1). These were identified in the midsagittal plane on color-coded FA maps. The middle cingulum portion was defined as the cingulum segment that lies between the anterior and posterior commissure, the anterior portion as the segment rostral to the anterior commissure, and the posterior portion as the segment caudal to the posterior commissure. The reproducibility of the cingulum reconstructions was assessed with intrarater reliability for one operator (J.S.) on a subset of 10 control brains with a 1 week interval between ratings.

Anterior cingulum. This section of the cingulum underlies the gray matter of the rostral or perigenual cingulate, BA 25, 32, 24 (Bush et al., 2000; Vogt, 2005). Five ROIs were used (Fig. 1*a*). The first waypoint OR ROI (blue) was drawn in the coronal plane, in line with the anterior commissure, and a second OR ROI in the axial plane at the most inferior region of the genu that could be seen in the axial plane. An AND ROI (green) was drawn in the coronal plane at the slice where the most posterior region of the genu can be visualized, and another AND ROI was drawn in the axial plane one contiguous slice dorsal to the second seed point. A NOT ROI (red) was drawn across the midline sagittal plane to exclude interhemispheric projections and further NOT ROIs were placed, when necessary, to exclude any outlier tracts that were not consistent with the known anatomy of the cingulum (Crosby et al., 1962; Schmahmann and Pandya, 2006). This procedure was repeated for the left and the right anterior cingulum.

Middle cingulum. This section of the cingulum underlies the gray matter of the midcingulate, BA 32′, 24′, 33′. Three ROIs were used (Fig. 1*b*). An AND ROI was drawn in the coronal plane, in line with the anterior commissure (identical to first OR ROI in the anterior cingulum). A second AND ROI was drawn in the coronal plane, in line with the posterior commissure. A NOT ROI was drawn across the midline sagittal plane to exclude interhemispheric projections and further NOT ROIs were placed, when necessary, to exclude any outlier tracts not consistent with the known anatomy of the cingulum (Crosby et al., 1962; Schmahmann and Pandya, 2006). This procedure was repeated for the left and the right middle cingulum.

Posterior cingulum. This section of the cingulum underlies the gray matter of the posterior cingulate cortex. A first waypoint OR ROI was drawn in the coronal plane in line with the posterior commissure (Fig. 1*c*). A second OR ROI was drawn in the axial plane at the most inferior slice where the full splenium can be seen in both hemispheres in the axial plane. An AND ROI was drawn in the coronal plane at the point where the splenium can first be seen in a coronal slice when moving anterior–posteriorly through the brain. A second AND ROI was drawn in the axial plane one contiguous slice dorsal to the second OR ROI. A NOT ROI was drawn across the midline sagittal plane to exclude interhemispheric projections and further NOT ROIs were placed, when necessary, to exclude any outlier tracts not consistent with the known anatomy of the cingulum (Crosby et al., 1962; Schmahmann and Pandya, 2006). This procedure was repeated for the left and the right posterior cingulum.

PHC. A waypoint ROI was placed on an axial slice level with the pons–midbrain junction around the cingulum fiber bundle (Fig. 1*d*). A NOT ROI was drawn across the midline sagittal plane to exclude interhemispheric projections. After visual inspection further NOT ROIs were placed, when necessary, to exclude projections to the occipital lobe and any outlier tracts not consistent with the known anatomy of the PHC (Crosby et al., 1962; Schmahmann and Pandya, 2006). This procedure was repeated for the left and the right PHC.

Reconstruction of fornix and corticospinal tract
The fornix was reconstructed according to previously published methods (Metzler-Baddeley et al., 2011). For the corticospinal tract, a waypoint OR ROI was drawn on an axial slice around the corticospinal tract rostral to the transverse pontine fibers in the brainstem (Fig. 1*f*). A NOT ROI was placed across the midsagittal plane to exclude interhemispheric projections. Another NOT ROI was drawn on a coronal slice posterior to the pons to exclude projections from the cerebellar peduncles, and any obvious outlier streamlines not consistent with the known corticospinal

tract anatomy were excluded using additional NOT ROIs. This procedure was repeated for the left and right corticospinal tract.

Statistical analysis
All statistical analyses were performed using SPSS 16.0 (SPSS). To allow the effects of healthy aging and disease to be evaluated separately, statistical analyses were based on raw rather than age-scaled scores.

Reproducibility was quantified with both the intraclass correlation coefficients (ICC) and coefficients of variation. ICC values of 0.60–0.79 are generally interpreted as representing substantial agreement between ratings. ICC values of 0.80–1.00 are generally interpreted as representing excellent agreement between ratings.

Differences in cingulum FA and MD were investigated using ANOVAs with the within factors "laterality" (left, right) and "cingulum segment" (anterior, middle, posterior, parahippocampal portion) and the between factor "group" (MCI patients, controls) and were explored *post hoc* with pairwise *t* tests, controlled for multiple comparison with Holm's correction.

The mean FA and MD for the different cingulum segments and the comparison pathways were correlated with individual scores in executive tasks by Pearson product–moment correlation coefficients, controlling for multiple-comparisons error with Bonferonni correction (corrected significance level of $\alpha \leq 0.0042$ for experiment-wise 5% significance level). Significant correlations were checked visually for outliers, defined as a datapoint >2 SD below or above the group mean. This criterion led to the exclusion of one healthy control's Category Fluency score, albeit not changing the pattern of results (correlation between FA in left anterior cingulum and Category Fluency before exclusion: $r = 0.63$; $p \leq 0.003$; after exclusion: $r = 0.71$; $p \leq 0.001$).

Finally, multivariate hierarchical regression analyses were used to account for potentially confounding effects of age, education, processing speed, and short-term memory span in the relationships between performance in cognitive control tasks and cingulum microstructure. The confounding variables (age, education, processing speed, visual span, and verbal span) were entered first in a stepwise fashion into the regression model, followed by the stepwise addition of the DTI indices (FA and MD separately) in the four cingulum segments (Bonferroni-corrected significance level, $p \leq 0.006$).

Results

Healthy volunteers and MCI patients were matched for age, education, premorbid intelligence, and gender ratio (Table 1).

Laterality and segment effects in the normal cingulum
The intrarater reproducibility of tract microstructural measures was very good. Intraclass correlation coefficients of ≥0.94 were achieved for all segments and both measures (FA and MD); no measure of intrarater coefficient of variation was >2.5%.

Both analyses of FA and MD revealed segment and laterality differences in cingulum microstructure. ANOVA revealed significant main effects for segment (FA: $F_{(3,87)} = 63.95$, $p \leq 0.001$; MD: $F_{(3,87)} = 23.15$, $p \leq 0.001$) and laterality (FA: $F_{(1,29)} = 5.44$, $p \leq 0.03$; MD: $F_{(1,29)} = 28.38$, $p \leq 0.001$) but not for MCI versus the controls (FA: $F_{(1,29)} = 0.32$, $p = 0.576$; MD: $F_{(1,29)} = 1.82$, $p = 0.187$).

Post hoc pairwise *t* tests, controlled for multiple comparison with Holm's correction, were used to investigate these effects further by testing differences for each left-right or adjacent segment pair. FA ($t_{(19)} = 4.5$, $p \leq 0.001$) was larger and MD lower ($t_{(19)} = 3.15$, $p \leq 0.0$) in the right relative to the left PHC but no laterality differences were found for other segments.

Differences in white matter microstructure were observed between all pairs of adjacent cingulum segments in both hemispheres with larger FA in middle relative to anterior cingulum (left: $t_{(19)} = 4.8$, $p \leq 0.001$; right: $t_{(18)} = 8.45$, $p \leq 0.001$, larger FA (left: $t_{(18)} = 4.6$, $p \leq 0.001$; right: $t_{(19)} = 2.9$, $p \leq 0.008$) and larger

Table 2. Correlations between control/executive measures and FA of cingulum segments in healthy control participants

	Anterior		Middle		Posterior		Parahippocampal		
	Left	Right	Left	Right	Left	Right	Left	Right	Fornix (comparison tract)
Digit Symbol Substitution Test	0.52*	0.36	−0.01	0.30	0.42	0.03	0.35	0.28	0.35
Stroop	0.48*	0.39	−0.02	0.30	0.66**[a]	0.37	0.18	−0.09	0.37
Category fluency	0.71***[a]	0.44	−0.10	0.19	0.37	0.21	0.04	−0.09	0.39
Verbal fluency	0.39	0.51*	0.17	0.18	0.33	0.27	−0.19	−0.46	0.17
Trails switching	−0.28	−0.32	0.04	−0.17	−0.35	−0.34	−0.06	−0.05	−0.12

Positive correlations indicate that better executive performance was associated with larger FA indices (i.e. more directional diffusion implying greater fiber coherence). Correlation coefficients are not shown for Tower of London rule violations because healthy participants made insufficient errors for these to be computed.

[a]Coefficients that reach experiment-wide significance based on Bonferroni correction ($p \leq 0.004$).

*$p \leq 0.05$, uncorrected; **$p \leq 0.01$, uncorrected; ***$p \leq 0.001$, uncorrected.

MD (left: $t_{(17)} = 5.6$, $p \leq 0.001$; $t_{(19)} = 4.8$, $p \leq 0.001$) in the middle relative to the posterior cingulum and larger FA (left: $t_{(18)} = 37.9$, $p \leq 0.001$; right: $t_{(19)} = 7.1$, $p \leq 0.001$) as well as lower MD (left: $t_{(17)} = 5.65$, $p \leq 0.001$; right: $t_{(19)} = 4.1$, $p \leq 0.001$) in the posterior compared with the PHC.

Cognitive control and white matter structure in healthy older adults

In healthy individuals, FA (but not MD) correlated with Category Fluency and Stroop Suppression, with both more strongly associated with FA in the left cingulum (Table 2). The relationship between left anterior cingulum FA and Category Fluency and left posterior cingulum FA and Stroop Suppression were significant at the experiment-wide Bonferroni-corrected level. Both these results, and the nonsignificant trends, show consistent laterality effects with stronger correlations in left-sided cingulum segments. No correlations were observed between cognitive measures and microstructure of control tracts (fornix, Table 2, or corticospinal tracts, data not shown).

In healthy participants, correlations with control tasks varied along the rostrocaudal extent of the cingulum. For Category Fluency and cingulum FA, the correlation coefficients were 0.71 in the anterior segment, but <0.4 in other segments (Table 2, Fig. 2). A similar pattern was present for the Digit Symbol Substitution Test. For Stroop Suppression, an additional association with FA of the left posterior cingulum segment was found (Fig. 2). Microstructure of the PHC was not associated with cognitive control tasks in normal healthy individuals.

The left lateralized and predominantly rostral pattern of correlation within the cingulum was unique to verbal and symbolic measures of cognitive control. General cognitive processing speed, in contrast, correlated most strongly with the middle segment of the cingulum with no clear laterality (left, $r = −0.654$, $p \leq 0.002$; right, $r = −0.663$, $p \leq 0.002$).

Cingulum microstructure in MCI and relation to cognitive control

ANOVA revealed no main effect of group (MCI vs healthy volunteers) on cingulum microstructure.

In the MCI group, the strongest relationships with performance were found for the MD measure (Table 3). Left lateralization of correlations with the verbal/symbolic control tasks was maintained in the patient group. Unlike healthy volunteers, patients made a number of rule violations on the Tower of London task. Rule violations correlated with both right and left anterior cingulum MD.

Regression analyses

To determine whether processing speed, or verbal and visual short-term memory span, might contribute to the association between cingulum microstructural indices and cognitive control, multivariate regression was performed. Cognitive variables were entered in a stepwise fashion, along with age and education, into a hierarchical regression model, followed by the stepwise addition of the microstructural indices (FA and MD) in the four cingulum segments.

For the controls, both visual span ($t = 3.38$, $p \leq 0.005$) and FA in the left anterior cingulum ($t = 3.5$, $p \leq 0.004$) made independent, approximately equal contributions to performance of the Digit Symbol Substitution Task. Variation of FA in the left anterior cingulum accounted for 20.5% (Digit Symbol), 44% (Category Fluency), and 41% (Stroop Suppression) of the variance in performance of cognitive control tasks not explained by age, education, and visual/verbal working memory.

In contrast, in patients with MCI, the relationships between anterior cingulum microstructure and cognitive control were mostly mediated by processing speed, which alone accounted for 55% of the variation in Digit Symbol performance. However, an independent contribution from MD in the left PHC emerged, which accounted for significant proportions of the variation in both Digit Symbol performance ($t = 4.55$, $p \leq 0.002$, accounting for a further 17% of the variance in performance) and rule violations in the Tower of London task ($t = 3.4$, $p \leq 0.006$, both significant at an experiment-wide Bonferroni-corrected level). The contribution of the left PHC to these tasks in MCI patients was independent of variation in both processing speed and visual/verbal working memory.

Discussion

Exploiting variations in white matter microstructure across two groups of older people, with and without early cognitive deterioration, made it possible to dissect the functional contribution of the cingulum to cognitive control. White matter microstructure varied across hemispheres and between adjacent cingulum segments. This anatomical discontinuity was expressed as relative functional specialization in relation to cognitive function. These segment differences presumably reflect the changing patterns of connectivity of the white matter throughout the length of the cingulum bundle. Performance on cognitive control tasks was highly sensitive to variations in microstructure of a subpopulation of fibers in the rostral cingulum. Further, there was evidence of hemispheric specialization, with the left rostral cingulum engaged especially in the context of verbal or symbolic rules (or "task set").

Like the cingulum, the fornix carries projections to the medial prefrontal cortex (Poletti and Creswell, 1977), yet fornix microstructure was not associated with cognitive control in either healthy individuals or patients. While both the fornix and cingulum innervate prefrontal regions (Mufson and Pandya, 1984; Morris et al., 1999), and even overlap in some sites, such as the
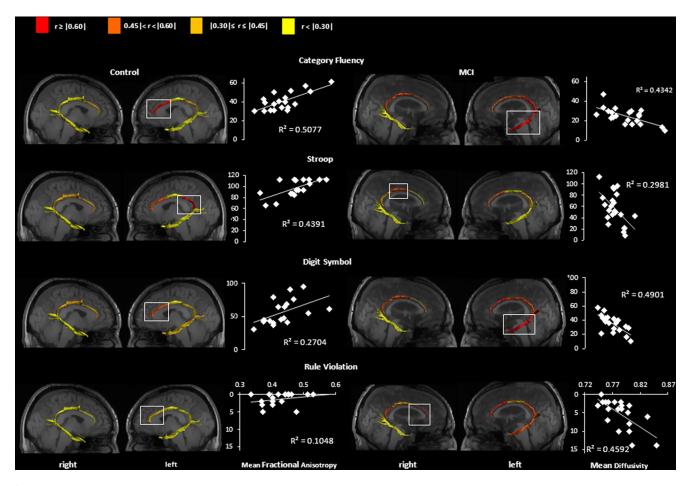
Figure 2. Parasagittal view of reconstructions of the four cingulum segments (anterior, middle, posterior, and parahippocampal) for the left and right hemisphere in the native space of one healthy participant (left) and one patient with MCI (right) coregistered to that individual's T1-weighted image. The cingulum segments are color coded to visualize the strength of the Pearson correlation coefficient between tract-specific diffusion metrics and performance in cognitive control tasks. Correlations highlighted by the white rectangles have the largest correlation coefficient for that measure and group and are further represented by scatter plots. Positive relationships for controls reflect that larger FAs were associated with better performance. Negative relationships in MCI reflect that larger MDs were associated with poorer performance. Note that for rule violations the scale on the y-axis has been inverted to make the direction of effect consistent across all tasks (this is an error score, so higher values reflect poorer performance).

Table 3. Correlations between control/executive measures and MD of cingulum segments in patients with MCI

	Anterior		Middle		Posterior		Parahippocampal		
	Left	Right	Left	Right	Left	Right	Left	Right	Fornix
Digit Symbol Substitution Test	−0.66**[a]	−0.45	−0.47*	−0.57**	−0.52*	−0.49*	−0.70***[a]	−0.17	0.14
Stroop	−0.53*	−0.19	−0.23	−0.55**	−0.40	−0.33	−0.21	−0.24	0.09
Rule violations	0.61**[a]	0.68***[a]	0.34	0.32	0.49*	0.48*	0.50*	0.11	−0.36
Category fluency	−0.47*	−0.46*	−0.46*	−0.58**	−0.66***[a]	−0.47*	−0.60**[a]	−0.08	0.34
Verbal fluency	0.01	0.07	−0.20	−0.23	−0.38	−0.15	−0.20	−0.11	−0.11
Trails switching	0.08	−0.02	0.18	0.27	0.18	0.20	0.22	0.15	0.20

Negative correlations indicate that lower executive performance was associated with larger tract diffusivity except for rule violations for which lower performance is reflected in a higher number of errors (i.e., a positive relationship with MD is expected).

[a]Coefficients that reach experiment-wide significance based on Bonferroni correction ($p \leq 0.004$).

*$p \leq 0.05$, uncorrected; **$p \leq 0.01$, uncorrected; ***$p \leq 0.001$, uncorrected.

subcallosal gyrus, these tracts comprise axons emanating from different structures, adding anatomical precision to the information that can be gleaned from the cingulum bundle functional correlations. Unlike the cingulum, the fornix was not segmented for analysis because fiber pathways do not leave the main body of the tract, only diverging at the level of the anterior commissure, where it cannot be reliably traced.

Investigation of microstructural variations introduced by aging (Michielse et al., 2010) or disease represents an extension of classical lesion studies. The quantitative nature of diffusion MRI

also allows the study of graded relationships, adding a degree of subtlety beyond simple dichotomous distinctions into individuals with or without focal injury. This approach complements studies in which lesions localized to the dorsal cingulum have been used to investigate networks for episodic memory (Lockhart et al., 2012). The disadvantage of this approach is that it might reduce the specificity of findings to the normal brain. However, this study provides a solution to this problem by using the fornix as a comparator tract. The fornix is highly susceptible to structural change in aging (Metzler-Baddeley et al., 2011) and MCI

(Bozoki et al., 2012) and has prefrontal cortex projections, albeit with a connectivity profile different from the cingulum (Poletti and Creswell, 1977). The results, therefore, offer a double dissociation, albeit relative: though no group effect was present in cingulum microstructure, variations in Tower of London performance introduced by disease were still specifically associated with cingulum rather than fornix microstructure.

Category Fluency, Color-Word Stroop, and Digit Symbol Substitution require rapid response generation according to specific task rules, which relate to either verbal or symbolic components of the tasks. All of these language-based control tasks were associated specifically with variation of left cingulum microstructure. In the Tower of London, however, verbal task rules relate to spatial rearrangements; for this task, associations were observed with both left and right cingulum. Maintenance of a set of task rules across multiple single responses is analogous to maintenance of task set in functional MRI paradigms (Dosenbach et al., 2006). One interpretation of the current findings is that the anterior segment of the cingulum provides the critical connections to dACC and that there is a degree of interhemispheric specialization of dACC connections, depending on whether task set relates to verbal or spatial rules. This functional lateralization has not been described previously, probably because of the limitations of fMRI, both in terms of spatial resolution and the necessity of spatial smoothing of coregistered imaging data. The left and right dACC are effectively contiguous, opposed in the midline, and therefore difficult to evaluate independently in smoothed, coregistered data (e.g., Fig. 4 in Dosenbach et al., 2006). As in previous studies based on DTI (Lockhart et al., 2012), we have been able to delineate distinct contributions of left and right cingulum, which in this case are likely to reflect hemispheric specialization within the dACC.

Although the dACC is closest anatomically to the anterior cingulum segment, an alternative interpretation is that connections to the more ventral medial prefrontal regions that form part of the default mode network (Raichle et al., 2001) are critical, although this would not explain the specificity of the association with executive control tasks. Further, the dACC itself harbors diverse functional subdivisions, contributing to motor as well as cognitive functions. The dACC includes three premotor regions, which in turn are connected to both prefrontal and primary motor cortex (Dum and Strick, 2002). The middle segment of the cingulum is the one likely to include the connections with more caudal premotor and motor cortical regions, while the anterior cingulum conveys connections to more rostral prefrontal sites. The tasks used here did not fully dissociate motor and cognitive contributions to the measure of "processing speed," but it is tempting to speculate that the bilateral relationship between middle cingulum and processing speed is due to ACC connections with more caudal motor regions (such as SMA and M1). An important goal of further studies will be to relate microstructure of specific subsets of connections with measures of connectivity within robust functional networks for higher-level control of movement and cognition (e.g., independent components that arise from analysis of fMRI covariance) (Damoiseaux et al., 2006; Smith et al., 2009).

In disconnection studies in monkey, the relevance of some connections only emerges when combinations of tracts are sectioned (Bachevalier et al., 1985; Gaffan et al., 2001). Similarly, the contribution of some connections to task performance may only become clear in the presence of compromise to other parts of a network. In patients with evidence of early cognitive decline, although strong univariate associations were present between anterior cingulum microstructure and both Digit Symbol Substitution and Tower of London performance, these relationships disappeared after controlling for variations in processing speed and working memory, unmasking an independent relationship between performance and microstructure of the left PHC. This relationship might reflect an increased reliance on cognitive processes other than working memory to support cognitive control: a candidate would be episodic memory accessed via PHC connections within the medial temporal lobe and possibly other connections within the dorsal cingulum (Lockhart et al., 2012). As mechanisms for maintenance of cognitive set fail, each response may necessitate a search of episodic memory for rule-relevant information with recruitment of different networks and connections.

The present study demonstrates that the efficacy of cognitive control in older adults is exquisitely sensitive to individual variations in cingulum microstructure. While these findings are likely to have corollaries in structure and function of prefrontal cortex, they illustrate how investigation of structural connectivity can capture interindividual variation and fine-grained distinctions in functional anatomy that are hard to resolve with other techniques (Dosenbach et al., 2006). The left anterior cingulum was particularly important for executive control involving verbal or symbolic task sets. Furthermore, in individuals with a degree of degradation of performance, it was possible to delineate independent contributions from more posterior connections (Fig. 2), suggesting that they become disproportionately important in response to the effects of disease. Information about the microstructure of ancillary connections might improve understanding of the genesis and potential compensation of deficits of cognitive control that occur in disorders that compromise the anterior cingulum, such as aging and neurodegenerative disease (Catheline et al., 2010).

References

Albert MS, DeKosky ST, Dickson D, Dubois B, Feldman HH, Fox NC, Gamst A, Holtzman DM, Jagust WJ, Petersen RC, Snyder PJ, Carrillo MC, Thies B, Phelps CH (2011) The diagnosis of mild cognitive impairment due to Alzheimer's disease: recommendations from the National Institute on Aging-Alzheimer's Association workgroups on diagnostic guidelines for Alzheimer's disease. Alzheimers Dement 7:270–279. CrossRef Medline

Alexander MP, Stuss DT, Picton T, Shallice T, Gillingham S (2007) Regional frontal injuries cause distinct impairments in cognitive control. Neurology 68:1515–1523. CrossRef Medline

Bachevalier J, Parkinson JK, Mishkin M (1985) Visual recognition in monkeys: effects of separate vs. combined transection of fornix and amygdalofugal pathways. Exp Brain Res 57:554–561. Medline

Bozoki AC, Korolev IO, Davis NC, Hoisington LA, Berger KL (2012) Disruption of limbic white matter pathways in mild cognitive impairment and Alzheimer's disease: a DTI/FDG-PET study. Hum Brain Mapp 33:1792–1802. CrossRef Medline

Bush G, Luu P, Posner MI (2000) Cognitive and emotional influences in anterior cingulate cortex. Trends Cogn Sci 4:215–222. CrossRef Medline

Catheline G, Periot O, Amirault M, Braun M, Dartigues JF, Auriacombe S, Allard M (2010) Distinctive alterations of the cingulum bundle during aging and Alzheimer's disease. Neurobiol Aging 31:1582–1592. CrossRef Medline

Crosby EC, Humphrey T, Lauer EW (1962) Correlative anatomy of the nervous system. New York: Macmillan.

Damoiseaux JS, Rombouts SA, Barkhof F, Scheltens P, Stam CJ, Smith SM, Beckmann CF (2006) Consistent resting-state networks across healthy subjects. Proc Natl Acad Sci U S A 103:13848–13853. CrossRef Medline

Dosenbach NU, Visscher KM, Palmer ED, Miezin FM, Wenger KK, Kang HC, Burgund ED, Grimes AL, Schlaggar BL, Petersen SE (2006) A core system for the implementation of task sets. Neuron 50:799–812. CrossRef Medline

Dum RP, Strick PL (2002) Motor areas in the frontal lobe of the primate. Physiol Behav 77:677–682. CrossRef Medline

Gaffan D, Parker A, Easton A (2001) Dense amnesia in the monkey after transection of fornix, amygdala and anterior temporal stem. Neuropsychologia 39:51–70. CrossRef Medline

Holroyd CB, Yeung N (2012) Motivation of extended behaviors by anterior cingulate cortex. Trends Cogn Sci 16:122–128. CrossRef Medline

Jones BF, Barnes J, Uylings HB, Fox NC, Frost C, Witter MP, Scheltens P (2006) Differential regional atrophy of the cingulate gyrus in Alzheimer disease: a volumetric MRI study. Cereb Cortex 16:1701–1708. Medline

Leemans A, Jones DK (2009) The B-matrix must be rotated when correcting for subject motion in DTI data. Magn Reson Med 61:1336–1349. CrossRef Medline

Lockhart SN, Mayda AB, Roach AE, Fletcher E, Carmichael O, Maillard P, Schwarz CG, Yonelinas AP, Ranganath C, Decarli C (2012) Episodic memory function is associated with multiple measures of white matter integrity in cognitive aging. Front Hum Neurosci 6:56. Medline

Metzler-Baddeley C, Jones DK, Belaroussi B, Aggleton JP, O'Sullivan MJ (2011) Frontotemporal connections in episodic memory and aging: a diffusion MRI tractography study. J Neurosci 31:13236–13245. CrossRef Medline

Metzler-Baddeley C, O'Sullivan MJ, Bells S, Pasternak O, Jones DK (2012) How and how not to correct for CSF-contamination in diffusion MRI. Neuroimage 59:1394–1403. CrossRef Medline

Michielse S, Coupland N, Camicioli R, Carter R, Seres P, Sabino J, Malykhin N (2010) Selective effects of aging on brain white matter microstructure: a diffusion tensor imaging tractography study. Neuroimage 52: 1190–1201. CrossRef Medline

Miller EK (2000) The prefrontal cortex and cognitive control. Nat Rev Neurosci 1:59–65. CrossRef Medline

Mioshi E, Dawson K, Mitchell J, Arnold R, Hodges JR (2006) The Addenbrooke's Cognitive Examination Revised (ACE-R): a brief cognitive test battery for dementia screening. Int J Geriatr Psychiatry 21:1078–1085. CrossRef Medline

Morris JC (1993) The Clinical Dementia Rating (CDR): current version and scoring rules. Neurology 43:2412–2414. CrossRef Medline

Morris R, Pandya DN, Petrides M (1999) Fiber system linking the mid-dorsolateral frontal cortex with the retrosplenial/presubicular region in the rhesus monkey. J Comp Neurol 407:183–192. CrossRef Medline

Mufson EJ, Pandya DN (1984) Some observations on the course and composition of the cingulum bundle in the rhesus monkey. J Comp Neurol 225:31–43. CrossRef Medline

Pasternak O, Sochen N, Gur Y, Intrator N, Assaf Y (2009) Free water elimination and mapping from diffusion MRI. Magn Reson Med 62:717–730. CrossRef Medline

Poletti CE, Creswell G (1977) Fornix system efferent projections in the squirrel monkey: an experimental degeneration study. J Comp Neurol 175:101–128. CrossRef Medline

Raichle ME, MacLeod AM, Snyder AZ, Powers WJ, Gusnard DA, Shulman GL (2001) A default mode of brain function. Proc Natl Acad Sci U S A 98:676–682. CrossRef Medline

Rushworth MF, Hadland KA, Gaffan D, Passingham RE (2003) The effect of cingulate cortex lesions on task switching and working memory. J Cogn Neurosci 15:338–353. CrossRef Medline

Schmahmann JD, Pandya DN (2006) Fiber pathways of the brain. New York: Oxford UP.

Smith SM, Fox PT, Miller KL, Glahn DC, Fox PM, Mackay CE, Filippini N, Watkins KE, Toro R, Laird AR, Beckmann CF (2009) Correspondence of the brain's functional architecture during activation and rest. Proc Natl Acad Sci U S A 106:13040–13045. CrossRef Medline

Tournier JD, Calamante F, Gadian DG, Connelly A (2004) Direct estimation of the fiber orientation density function from diffusion-weighted MRI data using spherical deconvolution. Neuroimage 23:1176–1185. CrossRef Medline

Vann SD, Aggleton JP, Maguire EA (2009) What does the retrosplenial cortex do? Nat Rev Neurosci 10:792–802. CrossRef Medline

Vogt BA (2005) Pain and emotion interactions in subregions of the cingulate gyrus. Nat Rev Neurosci 6:533–544. CrossRef Medline

Vogt BA, Finch DM, Olson CR (1992) Functional heterogeneity in cingulate cortex: the anterior executive and posterior evaluative regions. Cereb Cortex 2:435–443. CrossRef Medline